J Mater Sci (2011) 46:7223–7227
DOI 10.1007/s10853-011-5680-8

Preparation and characterization of mesoporous silicon spheres directly from MCM-48 and their response to ammonia

Jiang Zhu · Ruibin Liu · Jun Xu · Changgong Meng

Received: 3 March 2011 / Accepted: 1 June 2011 / Published online: 11 June 2011

Abstract The synthesis process of mesoporous silicon spheres directly from MCM-48 through a metal thermal reduction reaction is presented. The MCM-48 spheres were reduced in vacuum at 620 °C, with the spherical shape retained. The synthesized porous silicon spheres were confirmed as crystalline silicon by X-ray diffraction and transmission electron microscope. The silicon spheres have a microstructure different to those of etched silicon films by traditional method. The sample exhibited a slight red shift in PL spectrum after exposure to ammonia. This shift from 2.00 to 1.98 eV is ascribed to the Si–N adduct which disorder the space charge region in the semiconductor to weaken the quantum confinement effect. This design enables the syntheses of mesoporous nanocrystalline silicon spheres with multifarious three-dimensional shapes inherited from MCM-48 for sensor or optical applications.

Abbreviations

XRD	X-ray powder diffraction
SEM	Scanning electron microscope
TEM	Transmission electron microscope
HRTEM	High resolution TEM
SAED	Selected area electron diffraction
EDS	Energy dispersion spectrometer
PL	Photoluminescence
BET	Brunauer–Emmet–Teller
BJH	Barret–Joyner–Halendar

J. Zhu
School of Chemistry and Chemical Engineering,
Liaoning Normal University, Dalian 116029, China

R. Liu · J. Xu · C. Meng (✉)
Chemistry Department, Dalian University of Technology,
Dalian 116024, China
e-mail: cgmeng@dlut.edu.cn

Introduction

Porous silicon has attracted more and more attention for its excellent porous structure, optical property and electronic performance [1–3]. It has been attracting interests for many applications, such as sensors, optics, bio-material as well as energy containing material since it was found of photoluminescence (PL) at room temperature in 1990 [4]. Traditionally porous silicon was synthesized by etching process including electrochemical and chemical etching [5–7]. However, the analogical treatments result in similar structures, which may restrict the variety of structures and correlative applications. Various attempts have been adopted to prepare different structures and it is proved that displacement reaction is one of the highly effective and promising methods, through which some natural forms of SiO_2 including rice husks, diatom shells, and sands have been reduced to porous silicon [8–10]. Our studies focus on converting the pure silica molecular sieves into porous silicon. Compared with other natural forms, pure silica molecular sieves, a special group form of SiO_2, could be studied in system and it is helpful to understand the mechanism of structure forming by analyzing the changes from the regular pores and channels in molecular sieves to the pores in porous silicon [11, 12]. In this paper porous silicon spheres were obtained directly from pure silica MCM-48 by the magnesiothermal reduction process at 620 °C, during which the spherical shape and fine feature were well preserved. The structure in samples is very different from those by traditional etching method, which may be applied in the field of sensor or drug loading [8, 13]. In addition NH_3 was adsorbed into the sample and the changes occurred in PL spectrums has been discussed. The result will help to understand the origin and characteristics of this material.

Experimental

Preparation of pure silica MCM-48

Hexadecyltrimethylammonium bromide (4.8 g) was added to the solution composed of H_2O (75 g), ethanol (80 g), and aqueous ammonia (20 g, 40%). The solution was stirred at a rate of 400 rev/min for 10 min and then 7.0 g tetraethoxysilane (TEOS) was added. After the solution was stirred for 2 h at ambient temperature, it was filtrated and washed with deionized water. The product was dried at 100 °C for 30 min and calcinated at 550 °C for 3 h to remove the template.

Synthesis of porous silicon spheres

A mixture of magnesium powder and MCM-48 (0.18 g, molar ratio Mg: SiO_2 = 2: 1) was placed in a ceramic boat in a tube furnace. After the furnace was evacuated, the mixture was heated to 620 °C for 2 h. The products were collected and immersed in HCl solution (molar ratio of $HCl:H_2O:EtOH = 0.50:3.57:6.73$) for 6 h at room temperature to remove the magnesia and excessive Mg powder. The sample was then exposed to a HF solution (molar ratio of $HF:H_2O:EtOH = 0.70:0.74:5.92$) for 10 min to ensure that any oxide was eliminated completely. At last the obtained silicon granules were dried at 100 °C for 4 h.

Static adsorption of NH_3

The porous silicon spheres were placed in a sample bottle in a dryer. The dryer was blown by Ar (99.999%) and then evacuated to a pressure of 260 mmHg. NH_3 was introduced into the dryer until the pressure was about 395 mmHg and at last Ar was filled into 760 mmHg. The NH_3 was adsorbed for 2 h and the sample was analyzed immediately to obtain the PL spectrum.

Characterization

The sample was characterized by a Shimadzu XRD-6000 diffractometer with Cu Kα ($\lambda = 1.54060$ Å) radiation (40 kV, 30 mA). The morphologies were observed by a JSM-5600LV scanning electron microscope (5.0 kV) and a Philips Tecnai G^2 20 transmission electron microscope (200 kV). The PL emission spectrum was measured with a Perkin Elmer LS55 spectrometer using a xenon lamp as the excitation source. The N_2 adsorption–desorption isotherm was obtained by using a Micrometrics ASAP-2020 analyzer.

Results and discussion

The X-ray powder diffraction (XRD) pattern of the as-synthesized pure silica MCM-48 shown in Fig. 1a is identical to the one reported by Romero et al. [14]. The XRD pattern of product porous silicon is shown in Fig. 1b. Only sharp peaks of crystal silicon (pdf 27–1402) were observed, which demonstrated that the conversion from SiO_2 to crystal silicon was confirmed. The baseline is not very smooth due to the existence of little amount of amorphous phase [15].

The scanning electron microscope (SEM) image of pure silica MCM-48 is shown in Fig. 2a and plenty of smooth spheres congregated together with the diameter of about 500 nm. As revealed in Fig. 2b, after reduction and treatments the spherical shape and size were well preserved, and even the state of congregation of spheres was retained. Compared with MCM-48, but the surface of silicon spheres was a little rough. The modest temperature and appropriate reaction time prevent the shape from distorting and collapsing. Meanwhile, the formation of a magnesia phase intertwining with silicon also solidifies the framework of the spheres. As a result, the original shape is well preserved [8].

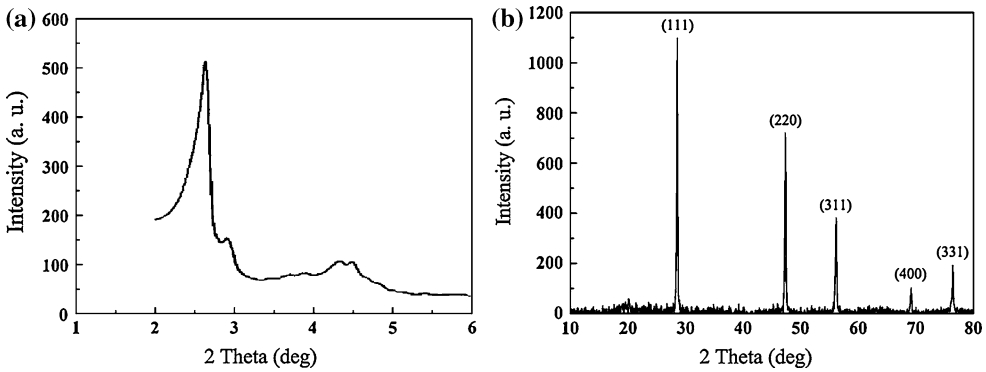

Fig. 1 XRD patterns of MCM-48 (**a**) and the as-synthesized porous silicon spheres (**b**)

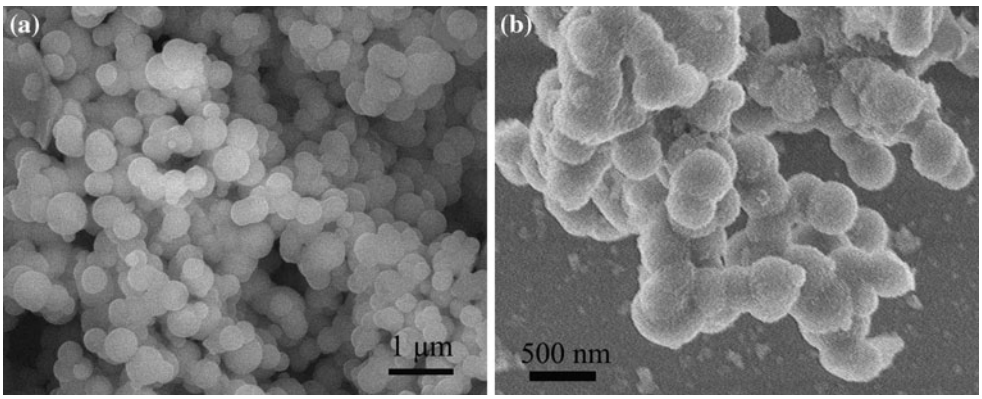

Fig. 2 SEM images of MCM-48 (**a**) and the as-synthesized porous silicon spheres (**b**)

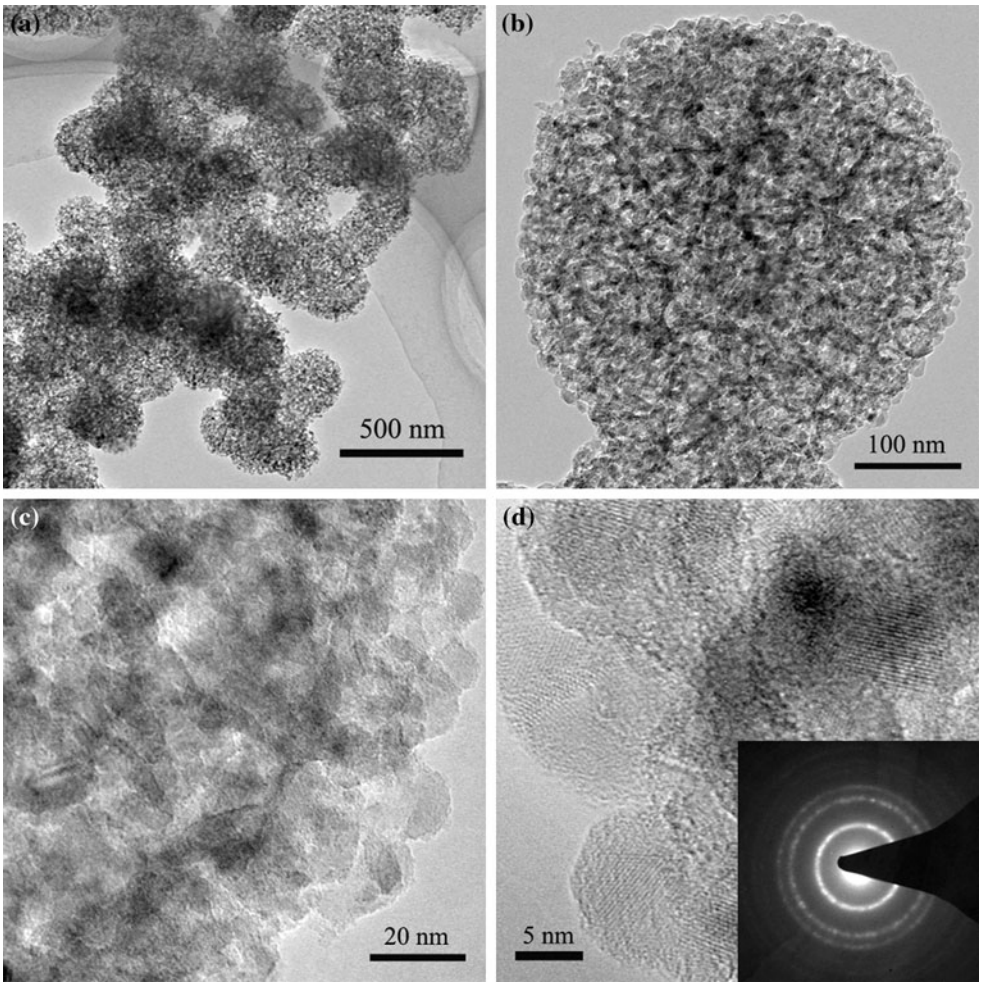

Fig. 3 TEM images of porous silicon spheres (**a**), a single silicon sphere (**b**), an amplified part on a sphere (**c**), and HRTEM image of porous silicon sphere (**d**), in the *inset* of **d** is the corresponding SAED patterns

The transmission electron microscope (TEM) image is presented in Fig. 3a. The spherical shape and the state of connecting spheres were well preserved. Figure 3b shows one silicon sphere with very loosen structure. In the amplified image shown in Fig. 3c there is many particles join together to form a three-dimensional structure. Most of the particles have a relatively uniform diameter of about 15–20 nm. Figure 3d shows a high resolution TEM (HRTEM) image and there are many crystalline silicon nanodots approximately 5 nm in diameter, indicated by

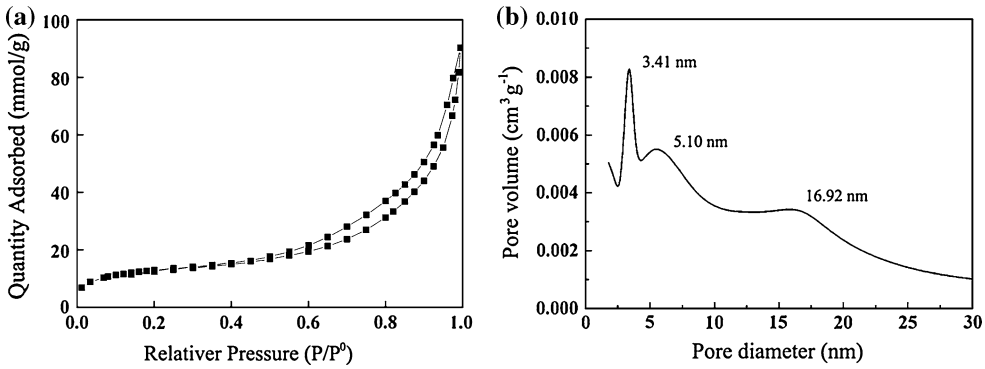

Fig. 4 Nitrogen adsorption–desorption isotherm of the porous silicon spheres (**a**) and the BJH pore size distribution (**b**)

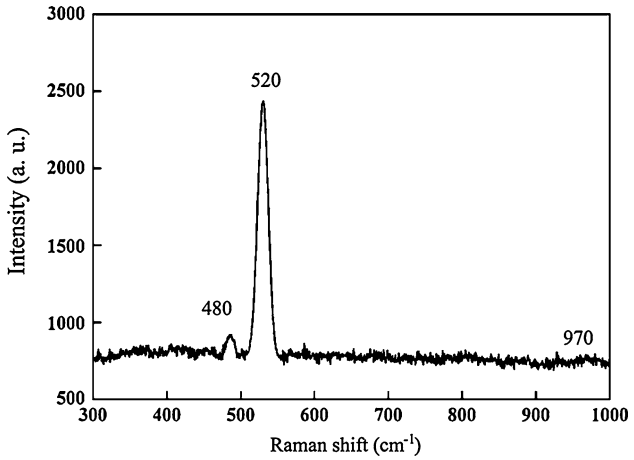

Fig. 5 Raman spectrum of porous silicon spheres

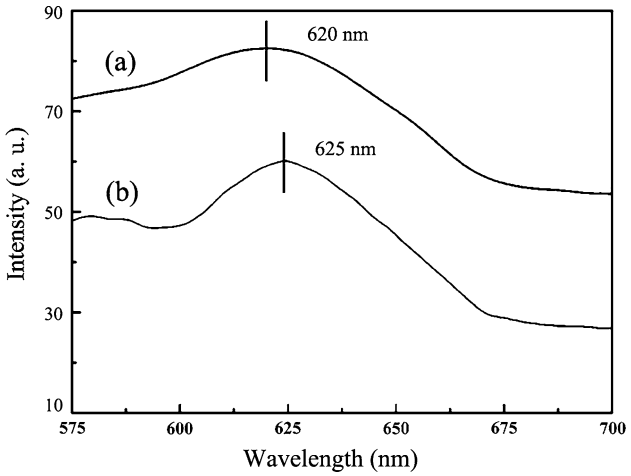

Fig. 6 Photoluminescence spectra of porous silicon spheres before (*a*) and after (*b*) NH_3 adsorption

the lattice fringes with different orientations. The interplanar spacing of the crystal state is about 0.32 nm, matching very well with the (111) planes of crystal silicon. The inset is the selected area electron diffraction (SAED) pattern in which well defined diffraction rings also match with polycrystalline silicon [16].

The N_2 adsorption–desorption isotherm of the sample was obtained at −196 °C and presented in Fig. 4a. The isotherm shows a representative type IIb curve with abrupt change in the relative pressure range of 0.8–0.9, which means that the mesoporosity only arises from particles interactions [17]. The hysteresis loop of type H3 occurs at the relative pressure range of 0.5–1.0, indicating the presence of narrow slit-like pores [18]. The Brunauer–Emmet–Teller (BET) report showed that the sample has a surface area of 43 $m^2\ g^{-1}$ and the single point pore volume is 0.109 $cm^3\ g^{-1}$ at a relative pressure of 0.976. The Barret–Joyner–Halendar (BJH) pore distribution is observed in Fig. 4b and there are three peaks centered at 3.41, 5.10, and 16.92 nm, respectively, bigger than that of MCM-48 (2.54 nm). The pore size distribution is calculated from the desorption branch, and then the peak at 3.41 nm may be an artifact due to the physical properties of the nitrogen. The change in pore diameter originates to the thermal contraction and defects of Si–Si bond from Si–O–Si bond, where the oxygen atom is seized by Mg. The relatively dispersed pore distribution is owing to the disordered collapse or lattice distortion in the phase change process [19].

Raman spectroscopy is very useful to gain structure information about bonding and disorder in porous silicon, because the wavenumbers and relative intensities of vibrations and phonons depended on the structure and chemical environment, as well as the structure and level of disorder are decisive to depolarization factors [9]. The Raman spectrum of the sample is shown in Fig. 5. The 520 cm^{-1} line can be assigned to crystal silicon, matching the observation in TEM [20]. The broadening of the 970 cm^{-1} line is ascribed to the second-order Raman scattering of TO mode at surface of crystal silicon or porous silicon [21]. Normally the 480 cm^{-1} line belongs to the amorphous silicon, matching the analysis to the XRD result. Thus we can propose that there exist little amount of amorphous silicon in the porous silicon sphere, due to the

solid-phase crystallization from amorphous SiO_2 to silicon takes place via the bond rearrangement process [21].

PL is the most important property for porous silicon. The PL spectrum of the sample was obtained at room temperature and labeled as curve a in Fig. 6. There is an emission centered at about 620 nm (2.0 eV), with an excitation at 315 nm. It is in the emission range of normal porous silicon (600–700 nm). After NH_3 adsorption, the band of 620 nm for porous silicon shifts to 625 nm (curve b in Fig. 6). Meanwhile in FTIR spectrum we found a new adsorption band of 1412 cm^{-1} after NH_3 adsorption, due to the vibration of $–NH^{3+}$ caused by the coupling between the surface of porous silicon and the nitrogen molecules [22]. The nitrides formed on the surface of porous silicon could efficiently disturb the space charge region in semiconductor, thus the quantum confinement effect resulted from the nanocrystalline silicon in the porous silicon was weakened, by which the little red shift in the PL spectrum was interpreted. More over, the steric effect from nitrogen molecules dynamically blocks the surface of porous silicon to a certain extent, which might also influence the light emission of porous silicon [23].

Conclusions

In general, mesoporous silicon spheres have been synthesized from MCM-48 by a thermal reduction reaction. The microstructure and possible mechanism for the formation have been discussed. NH_3 has been adsorbed by a static method and the changes in the PL spectra are considered to originate from the quantum confinement effect and the steric effect. This general approach has considerable promise for the further extensive study of the new structures of porous silicon.

Acknowledgements The authors are grateful to Experimental Center of Chemistry, Dalian University of Technology (China) for providing the necessities in experiments. Many thanks are dedicated to Mr. Jian Wu for his continuous help.

References

1. Torres-Costa V, Martin-Palma RJ (2010) J Mater Sci 45:2823. doi:10.1007/s10853-010-4251-8
2. Mizsei J (2007) Thin Solid Films 515:8310
3. Zhao Y, Li D, Sang W, Yang D, Jiang M (2007) J Mater Sci 42:8496. doi:10.1007/s10853-007-1749-9
4. Canham LT (1990) Appl Phys Lett 57(10):1046
5. Ohmukai M, Okada K, Tsutsumi Y (2005) J Mater Sci 16:119. doi:10.1007/s10854-005-6461-4
6. Zhao Y, Li D, Yang D (2006) J Mater Sci 41:5283. doi:10.1007/s10853-006-0267-5
7. Chuang SF, Collins SD, Smith RL (1989) Appl Phys Lett 55(7):675
8. Bao Z, Weatherspoon MR, Shian S, Cai Y, Graham PD, Allan SM, Ahmad G, Dickerson MB, Church BC, Kang Z, Abernathy HW III, Summers CJ, Liu M, Sandhage KH (2007) Nature 446:172
9. Hai NH, Grigoriants I, Gedanken A (2009) J Phys Chem C 113:10521
10. Banerjee HD, Sen S, Acharya HN (1982) Mater Sci Eng 52:173
11. Zhu J, Wang Y, Meng CG (2010) J Mater Sci 45:6769. doi:10.1007/s10853-010-4773-0
12. Zhu J, Liu RB, Xu J, Meng CG (2011) J Mater Sci 46:3840. doi:10.1007/s10853-011-5300-7
13. Guo M, Zou X, Ren H, Muhammad F, Huang C, Qiu S, Zhu G (2011) Microporous Mesoporous Mater 142:194
14. Romero AA, Alba MD, Zhou WZ, Klinowski J (1997) J Phys Chem B 101:5294
15. Bustarret E, Sauvaian E, Ligeon M, Rosenbauer M (1996) Thin Solid Films 276:134
16. Liu S, Kobayashi M, Sato S, Kimura K (2005) Chem Commun 37:4690
17. Huo Q, Zhao D, Feng J, Weston K, Buratto SK, Stucky GD, Schacht S, Schüth F (1997) Adv Mater 9:974
18. Hilonga A, Kim J, Sarawade PB (2010) J Mater Sci 45:1264. doi:10.1007/s10853-009-4077-4
19. Martin-Palma RJ, Pasual L, Herrero P, Martinez-Duart JM (2002) Appl Phys Lett 81:25
20. Yang S, Cai W, Zeng H, Li Z (2008) J Appl Phys 104:023516-1
21. Salcedo WJ, Fernandez FJR, Rubim JC (1999) J Raman Spectrosc 30:29
22. Li GB, Hou XY, Yuan S, Chen HJ, Zhang FL, Fan HL, Wang X (1996) J Appl Phys 80(10):5967
23. Chandler-Henderson RR, Sweryda-Krawiec B, Coffer JL (1995) Phys Chem 99:8851